Comparison of methods for achieving induced transparency or absorption with pulse delay or advancement in a single microresonator

A. T. Rosenberger*
Department of Physics, Oklahoma State University, Stillwater, OK, USA 74078-3072

ABSTRACT

Induced transparency and absorption effects can be observed in the throughput of an optical microresonator that has two coresonant modes with very different quality factors. There are several different methods for achieving these effects, which enable slow light and fast light, i.e., the delay or advancement of an incident resonant pulse. For example, mode coupling can be employed. This coupling can take place between modes of the same polarization or modes of orthogonal polarization. Another method is based on superposition, when two orthogonally polarized modes are driven simultaneously by linearly polarized input light and throughput of the same polarization as the input is detected. In general, induced transparency is accompanied by pulse delay, whereas induced absorption can be accompanied by pulse advancement or delay. A number of different methods for producing induced transparency or absorption are compared here. Several properties are considered for comparison. One involves the widths of the induced transparency or absorption window and of the corresponding spectral region of steep dispersion. Achievable pulse delays or advancements, along with pulse distortion and delay-bandwidth (or advancement-bandwidth) products, are also compared. Different methods allow for different amounts of control over various system parameters, and these are compared as well. The differences among the several methods are evaluated in consideration of suitability for employment in various applications.

Keywords: slow light, fast light, microresonator, whispering-gallery modes

1. INTRODUCTION

The throughput of a single microresonator can exhibit induced transparency or induced absorption effects. For example, these can be observed when tunable laser light is injected via a tapered-fiber coupler into a dielectric microresonator such as a fused-silica hollow bottle resonator (HBR) that has two coresonant (frequency-degenerate) whispering-gallery modes (WGMs) having very different quality factors (Qs).[1] Induced transparency is generally accompanied by pulse delay (slow light), whereas induced absorption can show pulse delay or pulse advancement (fast light). Three methods involving a pair of copropagating WGMs will be considered here. Coresonance can happen by coincidence, but it can also be introduced in a controllable way by strain tuning (axial stretching of the HBR). Whispering-gallery microresonators have two orthogonally polarized families of modes, TE (transverse electric) and TM (transverse magnetic). Because the birefringence induced by strain tuning causes the two types of modes to tune at different rates, it can be used to impose frequency degeneracy between a TE mode and a TM mode.[2-4] Strain tuning also causes WGMs of the same polarization but different radial orders to frequency-shift at different rates, and can be used to make them coresonant.[5-7]

The first method for achieving induced transparency and absorption uses cross-polarization coupling (CPC). Light of one polarization circulating in a WGM of the microresonator can be coupled into a coresonant WGM of the orthogonal polarization. This CPC is likely a result of weak polarization rotation, but for our purposes it can be treated as weak scattering. In this case, the input light and detected throughput is one polarization, say TE. Because of CPC, the interaction with a coresonant TM WGM produces a throughput spectrum (as the driving laser is scanned in frequency) showing cross-polarization coupled-mode induced transparency and absorption (CMIT, CMIA).[8,9] An input pulse whose center frequency is resonant will be delayed or advanced. These effects are similar to the coupled-resonator-induced transparency and absorption (CRIT, CRIA) observed in coupled whispering-gallery microresonators,[10,11] except that output from the non-driven WGM can also be detected here.

*atr@okstate.edu; phone 1 405 744-6742; fax 1 405 744-6811; physics.okstate.edu/rosenber/index.html

Slow Light, Fast Light, and Opto-Atomic Precision Metrology IX, edited by Selim M. Shahriar, Jacob Scheuer, Proc. of SPIE Vol. 9763, 97631E · © 2016 SPIE
CCC code: 0277-786X/16/$18 · doi: 10.1117/12.2220237

In the case of CMIT and CMIA, the light incident on the microresonator is linearly polarized so as to directly excite only one family of modes, say TE, and the mode coupling effects are observed as a splitting or modification of the shape of the resonant TE throughput dip. The second method uses incident light linearly polarized at 45° (for example) in the TE-TM basis to drive coresonant modes of the two polarizations and produce induced transparency or absorption in the throughput of the same linear polarization as the incident light. This occurs even in the absence of cross-polarization mode coupling, demonstrating that mode superposition is sufficient to produce these effects, including pulse delay or advancement. The effects induced in this manner are referred to as coresonant polarization induced transparency and absorption (CPIT, CPIA).[8,9]

For the third method, linearly polarized light is input and excites only TE (or TM) modes; two modes, of like polarization but different radial order, are coresonant and coupled to each other. In this case, the coupling between modes is mediated by the input/output coupling fiber – light circulating in one WGM couples out into the fiber and then immediately back into the other WGM.[5,12,13] We use FMIT and FMIA to refer to the fiber-mediated induced transparency and absorption effects seen using this method.

A simple ring-cavity model has been used to study the effects observed in the three methods. Numerical application of the model can be used to produce plots that can be used for comparison with experimental results.[1] In this work, however, the emphasis will be on analytical results that can be used to compare the three methods. The main results to be presented here are for the width of the transparency window and for the group delay or advancement.

2. MODEL

Physical insight into IT and IA in a single microresonator can be gained by using a simplified model based on a ring cavity. The model based on the cavity sketched in Fig. 1 is designed for CMIT/CMIA with cross-polarization mode coupling. With minor modifications, it can be used for all three methods studied here; comments on how to do this in each case will be presented in the discussion below.

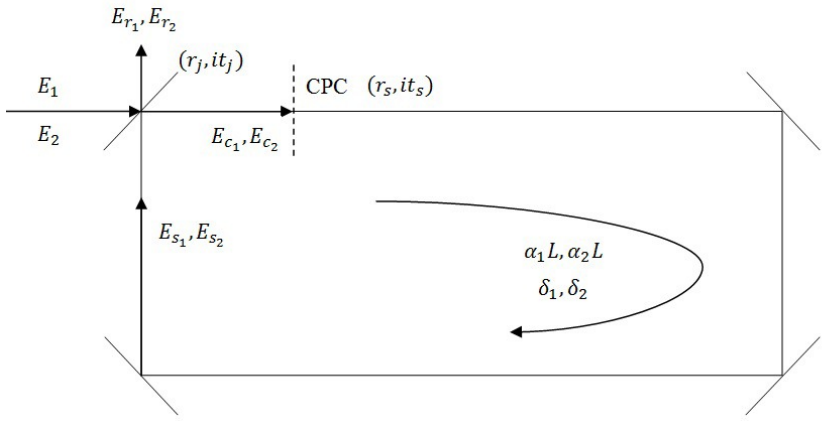

Figure 1. Ring cavity model. Two input fields are injected into the resonator, where they couple to each other. The net reflected fields are analogous to the throughput fields in a whispering-gallery microresonator system. The labeled fields and system parameters are defined and discussed in the following text.

For cross-polarization coupling (CPC), the E_j (j = 1,2) are orthogonal polarization components of the input field. Input/output coupling occurs at the partial reflector, which has reflection and transmission coefficients r_j and it_j; this partial reflector is assumed to be ideal, so that $R_j+T_j = 1$, where $R_j = r_j^2$ and $T_j = t_j^2$. Immediately after the fields enter the cavity, CPC (modeled here as cross-polarization scattering) takes place with an amplitude it_s. Thus, $T_s = t_s^2 = 1 - r_s^2$ is the CPC probability per round trip, and is the measure of intermodal coupling strength. The intracavity fields of the two orthogonally polarized modes just before and just after the input/output coupler are E_{s_j} and E_{c_j}, respectively. In

propagating one intracavity round trip of length L, the fields undergo intrinsic losses $\alpha_j L$ and accumulate phases δ_j. The E_{r_j} denote the throughput fields, which are given by

$$E_{r_1} = r_1 E_1 + i t_1 E_{s_1} \quad \text{and} \quad E_{r_2} = r_2 E_2 + i t_2 E_{s_2}. \tag{1}$$

The intracavity fields satisfy these differential equations:

$$\begin{aligned} \dot{E}_{s_1} &= -\gamma_1 E_{s_1} + \frac{i t_s}{\tau_{rt_1}} E_{s_2} + \frac{i t_1}{\tau_{rt_1}} E_1 - \frac{t_2 t_s}{\tau_{rt_1}} E_2, \\ \dot{E}_{s_2} &= -\gamma_2 E_{s_2} + \frac{i t_s}{\tau_{rt_2}} E_{s_1} + \frac{i t_2}{\tau_{rt_2}} E_2 - \frac{t_1 t_s}{\tau_{rt_2}} E_1, \end{aligned} \tag{2}$$

where the τ_{rt_j} are the round-trip times in the two modes. WGMs of different orders or different polarizations can have different effective refractive indices, hence different propagation constants and different round-trip times, even when they have the same frequency. Substituting Eqs. (2) into the time derivatives of Eqs. (1) then gives the differential equations for the throughput fields. In Eqs. (2), the complex decay rates γ_j are given by

$$\gamma_j = \frac{T_j + \alpha_j L}{2\tau_{rt_j}} - i\frac{\delta_j}{\tau_{rt_j}} + \frac{T_s}{2\tau_{rt_j}} = \kappa_j\left(1 + i\theta_j\right) + \frac{T_s}{2\tau_{rt_j}}, \tag{3}$$

where κ_j is one-half the inverse cavity (photon) lifetime of mode j and θ_j is the detuning of the resonant frequency of mode j from the input frequency in units of half the mode linewidth. Note that the quality factor of mode j can be written as $Q_j = \omega_j \tau_j = \omega_j / \left(2\kappa_j\right)$, where ω_j is mode j's resonant frequency and τ_j its photon lifetime. When the model is solved numerically, the possibility of a slight offset from coresonance between the two modes is allowed. For CMIT and CMIA, only one input field is nonzero, and only the throughput corresponding to that polarization is observed. The CPC strength T_s is treated as a free parameter determined by fitting to experimental results. Examples of numerical results are shown in the following two figures.

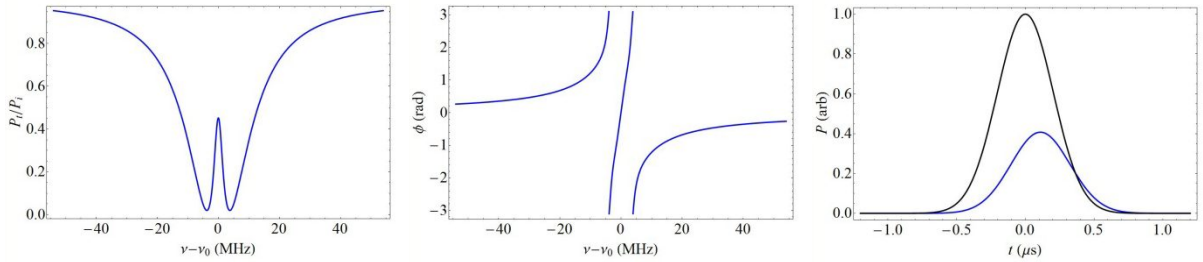

Figure 2. CMIT (CPC). Left to right: steady-state throughput power spectrum, steady-state dispersion, pulse response – input Gaussian pulse in black and delayed throughput pulse in blue.

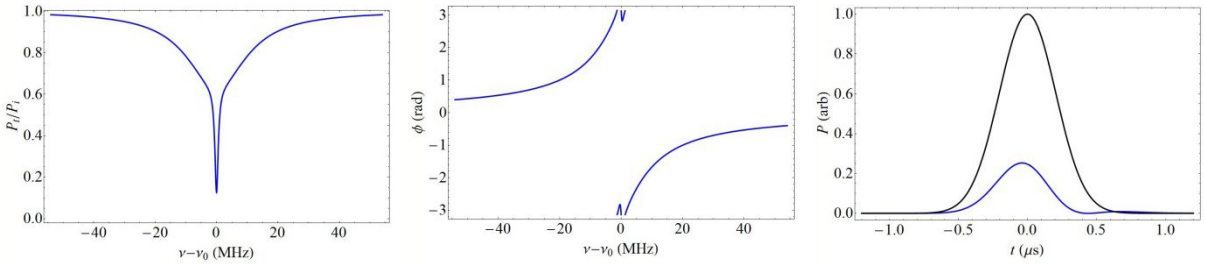

Figure 3. CMIA (CPC). Left to right: steady-state throughput power spectrum, steady-state dispersion, pulse response – input Gaussian pulse in black and advanced throughput pulse in blue.

In Figs. 2 and 3, $E_2 = 0$; then for different combinations of system parameters, $\left|\frac{E_{r_1}(\delta_1)}{E_1}\right|^2$ (when δ_1 is converted into the detuning of the input frequency from the coresonance frequency) is the throughput power spectrum. Dispersion is given by the phase of the throughput relative to the input: $\phi(\delta_1)$ in $\frac{E_{r_1}(\delta_1)}{E_1} = \left|\frac{E_{r_1}(\delta_1)}{E_1}\right| \exp(i\phi(\delta_1))$; also, $1 - \left|\frac{E_{r_1}(\delta_1)}{E_1}\right|^2$, by analogy to the probe absorption spectrum in EIT,[14] allows an expression for the IT spike width to be found. The resonant dispersion slope is proportional to the group delay (or advancement, if negative) as will be discussed in the Results section below.

To apply the model to CPIT and CPIA, the input field is $E_i = (E_1 + E_2)/\sqrt{2}$ with E_1 and E_2 taken to be equal (45° linear polarization), $T_s = 0$, and the throughput field is $E_r = (E_{r_1} + E_{r_2})/\sqrt{2}$. For FMIT and FMIA, there is only one input field (E_i) and one throughput field (E_r), but two intracavity fields. The input/output coupling loss coefficients it_j describe coupling from the input field into each intracavity mode and from each intracavity mode into the throughput field. In this case, the intermodal coupling amplitude it_s is replaced by $-t_1\, t_2/2$.[5,12,13]

3. RESULTS

Some analytical results from the model are presented in this section. Unless noted otherwise, it will be assumed that $Q_1 << Q_2$, and the most common limit to be considered will be the one in which both WGMs are strongly overcoupled. The coupling regime is described in terms of the ratio of coupling loss to intrinsic loss, $x_j = T_j / \alpha_j L$; a ratio < 1 denotes undercoupling, a ratio = 1 indicates critical coupling, and a ratio > 1 means overcoupling. Strong overcoupling thus implies $x_j >> 1$. The quality factor Q_j is inversely proportional to the total loss:

$$Q_j = \frac{4\pi^2 na}{\lambda(T_j + \alpha_j L)} = \frac{\nu}{\Delta\nu_j}, \tag{4}$$

where n is the effective refractive index of the mode, a is the resonator radius, and λ and ν are the wavelength and frequency of the light. The WGM linewidth $\Delta\nu_j$ is thus proportional to the total loss.

The model is solved in steady state to find the ratio of the (complex) throughput field to the (assumed real) input field. This ratio is then used as outlined in the previous section to find the throughput spectrum and dispersion as functions of the detuning of the input frequency from resonance. Since the difference in the refractive indices of the two modes is small, we take them to have the same effective n, implying that the phase detunings can be taken to be equal, and so

$$\delta_1 = \delta_2 = \delta = \frac{4\pi^2 na}{c}(\nu - \nu_0) \tag{5}$$

gives the relation of δ to the frequency detuning $\nu - \nu_0$. Note from Eqs. (4) and (5) that the WGM linewidth in phase is simply equal to the total loss: $\Delta\delta_j = T_j + \alpha_j L$.

3.1 Transparency window (throughput spike) width

For the case of CMIT, the following result is obtained for the inverted throughput spectrum:

$$1 - \left|\frac{E_{r_1}(\delta)}{E_1}\right|^2 = \frac{T_1\alpha_1 L}{\left(\delta - \frac{T_s}{\delta}\right)^2 + \left(\frac{T_1 + \alpha_1 L}{2}\right)^2}. \tag{6}$$

Note that it has not been necessary to assume strong overcoupling here. By analogy with the similar expression for the probe absorption coefficient in EIT, the phase width of the transparency window is seen to be

$$\Delta\delta_{IT} = \frac{4T_s}{T_1 + \alpha_1 L}. \tag{7}$$

For typical values of T_s, the frequency width of the transparency window will be the same order of magnitude as the width of the higher-Q WGM ($\Delta\nu_2$). It may be slightly smaller, but not orders of magnitude smaller.

In the case of CPIT, $T_s = 0$; for both WGMs strongly overcoupled, we find

$$1 - \left|\frac{E_r(\delta)}{Ei}\right|^2 = \frac{T_1/2}{\left(\delta - \frac{T_1 T_2}{4\delta}\right)^2 + \left(\frac{T_1}{2}\right)^2} \tag{8}$$

and

$$\Delta\delta_{IT} = T_2. \tag{9}$$

This is exactly the width of the higher-Q WGM. In comparison to CMIT with strong overcoupling, where the intrinsic loss in Eq. (7) becomes negligible, it is as if the intermodal coupling strength T_s has been replaced by $T_1T_2/4$. Interestingly, as noted at the end of Section 2, this is just what happens in FMIT.

However, when FMIT is considered, for both WGMs strongly overcoupled and with equal throughput dip depths, so that $x_1 = x_2$, the result is

$$1 - \left|\frac{E_r(\delta)}{Ei}\right|^2 = \frac{2T_1\alpha_2 L}{\left(\delta - \frac{T_1\alpha_2 L}{2\delta}\right)^2 + \left(\frac{T_1}{2}\right)^2} \tag{10}$$

and

$$\Delta\delta_{IT} = 2\alpha_2 L. \tag{11}$$

This width is now significantly less than the width of the higher-Q WGM (T_2), because the mode is strongly overcoupled. Thus FMIT has the potential to produce the narrowest transparency windows.

3.2 Group delay

The group delay is given in terms of the dispersion; specifically, it is proportional to the slope of the phase of the throughput with respect to the input, evaluated on resonance:

$$\tau_g = \frac{2\pi n a}{c}\left.\frac{d\phi}{d\delta}\right|_{\delta=0}, \tag{12}$$

where $\phi(\delta)$ is defined as in Section 2.

For the case of CMIT/CMIA, the following expression is found for the slope in the limit where both WGMs are strongly overcoupled:

$$\left.\frac{d\phi}{d\delta}\right|_{\delta=0} = \frac{T_1 T_s - \frac{T_1 T_2^2}{4}}{T_s^2 - \left(\frac{T_1 T_2}{4}\right)^2} \xrightarrow[T_2 \to 0]{} \frac{T_1}{T_s}, \tag{13}$$

where the small-T_2 limit corresponds to the case presented in Eqs. (6) and (7). From the full expression, it can be seen that the group delay will be negative, and there will be pulse advancement, for the CPC strength within the range satisfying

$$\frac{T_2^2}{4} < T_s < \frac{T_1 T_2}{4}. \tag{14}$$

For other values of T_s, there will be pulse delay.

In the case of CPIT/CPIA with 45° linear polarization, but no assumptions as to the input/output coupling regimes or Q values of the two WGMs, the dispersion is

$$\left.\frac{d\phi}{d\delta}\right|_{\delta=0} = 2\frac{\frac{x_1^2}{T_1}(x_2+1)^2 + \frac{x_2^2}{T_2}(x_1+1)^2}{(x_1+1)(x_2+1)(x_1x_2-1)}, \tag{15}$$

which goes to $2/T_2$ if both WGMs are strongly overcoupled and $Q_2 >> Q_1$, as in Eqs. (8) and (9). Equation (15) shows that the condition for pulse advancement in this case is simply

$$x_1 x_2 < 1. \tag{16}$$

For FMIT/FMIA, with no assumptions as to the input/output coupling regimes or Q values of the two WGMs, the dispersion is

$$\left.\frac{d\phi}{d\delta}\right|_{\delta=0} = 4\frac{\frac{x_1^2}{T_1} + \frac{x_2^2}{T_2}}{(x_1+x_2)^2 - 1}. \tag{17}$$

In the limit of both WGMs strongly overcoupled with equal throughput dip depths so that $x_1 = x_2$, and $Q_2 >> Q_1$, as in Eqs. (10) and (11), this goes to $1/T_2$. In general, the condition for pulse advancement in this case is

$$(x_1+x_2)^2 < 1. \tag{18}$$

For the three IT cases, if we take the pulse bandwidth to be equal to the transparency window width, the delay-bandwidth products are given by

$$\tau_g \Delta\nu_{IT} = \frac{1}{2\pi}\Delta\delta_{IT}\left.\frac{d\phi}{d\delta}\right|_{\delta=0} = \begin{cases} 2/\pi \text{ for CMIT} \\ 1/\pi \text{ for CPIT} \\ 1/(x_2\pi) \text{ for FMIT} \end{cases}. \tag{19}$$

4. DISCUSSION

First, let's summarize the comparison of the three methods. FMIT has the narrowest transparency window but the smallest delay-bandwidth product. CMIT and CPIT are comparable in these two respects, but CMIT relies on having intermodal coupling as a result of CPC. The strength of (or even existence of) CPC is not predictable for any given pair of coresonant orthogonal WGMs, as it likely depends on details of the spatial overlap (and perhaps phase matching) of the two modes. It's easy to find coresonance, however, so with no (or weak) CPC, CPIT can always be found. Since CPIT also permits tuning of the pulse delay by changing the polarization angle of the input light,[8] it seems to be the most versatile method for achieving and using induced transparency effects with a single resonator.

The strong reduction of the delay-bandwidth product for FMIT, compared to the other two methods, is a distinctive feature. It raises the question of whether a system could be designed to have a large factor such as x_2 in the numerator rather than in the denominator. An enhanced delay-bandwidth product would be very useful for applications.

It is hoped that one or all of these three methods for using interacting (or at least superimposed) WGMs of a single resonator can contribute to enhanced techniques for sensing. Chemical sensing can be done using frequency-shift or amplitude-change[15] approaches, and fast light (pulse advancement) may be useful for enhancing the response of optical gyroscopes.[16] Of the three methods, CMIA has the strongest constraint on achieving fast light; again, the advantage here goes to CPIA for induced absorption effects with a single resonator.

REFERENCES

[1] Bui, K. V. and Rosenberger, A. T., "Experimental study of induced transparency or absorption and slow or fast light using orthogonally polarized whispering-gallery modes of a single microresonator," Proc. SPIE 9763 (in press).

[2] Ilchenko, V. S., Volikov, P. S., Velichansky, V. L., Treussart, F., Lefèvre-Seguin, V., Raimond, J.-M., and Haroche, S., "Strain-tunable high-*Q* optical microsphere resonator," Opt. Commun. 145, 86-90 (1998).

[3] von Klitzing, W., Long, R., Ilchenko, V. S., Hare, J., and Lefèvre-Seguin, V., "Tunable whispering gallery modes for spectroscopy and CQED experiments," New Journal of Physics 3, 14.1-14.14 (2001).

[4] Rezac, J. P. and Rosenberger, A. T., "Locking a microsphere whispering-gallery mode to a laser," Opt. Express 8, 605-610 (2001).

[5] Yang, Y., Saurabh, S., Ward, J., and Nic Chormaic, S., "Coupled-mode-induced transparency in aerostatically tuned microbubble whispering-gallery resonators," Opt. Lett. 40, 1834-1837 (2015).

[6] Henze, R., Seifert, T., Ward, J., and Benson, O., "Tuning whispering gallery modes using internal aerostatic pressure," Opt. Lett. 36, 4536-4538 (2011).

[7] Carmon, T., Schwefel, H. G. L., Yang, L., Oxborrow, M., Stone, A. D., and Vahala, K. J., "Static Envelope Patterns in Composite Resonances Generated by Level Crossing in Optical Toroidal Microcavities," Phys. Rev. Lett. 100, 103905 (2008).

[8] Rosenberger, A. T., "EIT analogs using orthogonally polarized modes of a single whispering-gallery microresonator," Proc. SPIE 8636, 863602-1—863602-11 (2013).

[9] Rosenberger, A. T., "Effects of polarization mode coupling and superposition in a whispering-gallery microresonator," Proc. SPIE 8998, 899813-1—899813-8 (2014).

[10] Smith, D. D., Chang, H., Fuller, K. A., Rosenberger, A. T., and Boyd, R. W., "Coupled-resonator-induced transparency," Phys. Rev. A. 69, 063804 (2004).

[11] Naweed, A., Farca, G., Shopova, S. I., and Rosenberger, A. T., "Induced Transparency and Absorption in Coupled Whispering-Gallery Microresonators," Phys. Rev. A 71, 043804 (2005).

[12] Dong, C.-H., Zou, C.-L., Xiao, Y.-F., Cui, J.-M., Han, Z.-F., and Guo, G.-C., "Modified transmission spectrum induced by two-mode interference in a single silica microsphere," J. Phys. B 42, 215401 (2009).

[13] Li, B.-B., Xiao, Y.-F., Zou, C.-L., Liu, Y.-C., Jiang, X.-F., Chen, Y.-L., Li, Y., and Gong, Q., "Experimental observation of Fano resonance in a single whispering-gallery microresonator," Appl. Phys. Lett. 98, 021116 (2011).

[14] Fleischhauer, M., Imamoglu, A., and Marangos, J. P., "Electromagnetically induced transparency: Optics in coherent media," Rev. Mod. Phys. 77, 633-673 (2005).

[15] Zhou, X., Zhang, L., Armani, A. M., Liu, J., Duan, X., Zhang, D., Zhang, H., and Pang, W., "An Integrated Photonic Gas Sensor Enhanced by Optimized Fano Effects in Coupled Microring Resonators With an Athermal Waveguide," J. Lightwave Technol. 33, 4521-4530 (2015).

[16] Smith, D. D., Chang, H., Myneni, K., and Rosenberger, A. T., "Fast-light enhancement of an optical cavity by polarization mode coupling," Phys. Rev. A 89, 053804 (2014).